

# EFFECT OF AMBIENT AND TYRE TEMPERATURE ON TRUCK TYRE ROLLING RESISTANCE

Jukka Hyttinen<sup>1,2)\*</sup>, Matthias Ussner<sup>1)</sup>, Rickard Österlöf<sup>1)</sup>, Jenny Jerrelind<sup>2)</sup> and Lars Drugge<sup>2)</sup>

<sup>1)</sup>Scania CV AB, Granparksvägen 10, Södertälje 15148, Sweden

<sup>2)</sup>ECO<sup>2</sup> Vehicle Design, Engineering Mechanics, KTH Royal Institute of Technology, Stockholm 10044, Sweden

(Received 10 January 2022; Revised 28 March 2022; Accepted 29 March 2022)

**ABSTRACT**—Rolling resistance is consuming a large portion of the generated powertrain torque and thus have a substantial effect on truck energy consumption and greenhouse gas emissions. EU labelling of tyres mandates the manufacturers to measure rolling resistance at +25 °C ambient temperature after stabilised rolling resistance has been established. This is a convenient way of comparing rolling resistance but disregards aspects such as transient rolling resistance and influence of the ambient temperature. For many purposes, such as dimensioning batteries for electric vehicles, this value is not representative enough to give a good understanding of the rolling resistance. In this article, the rolling resistance of a truck tyre was measured at different ambient temperatures (-30 to +25 °C) in a climate wind tunnel and a considerable tyre and ambient temperature dependency on rolling resistance was found. The investigation shows that the temperature inside the tyre shoulder has a good correlation with rolling resistance. Measurements with spraying water on tyres were conducted showing a considerable increase in rolling resistance due to higher cooling effect. Driving range simulations of a long haulage battery-electric truck have been conducted with temperature-dependent rolling and aerodynamic resistance, showing a significant decrease in driving range at decreasing temperature.

**KEY WORDS** : Truck tyre, Rolling resistance, Climate wind tunnel, Ambient temperature, Tyre temperature, Battery-electric truck range

## NOMENCLATURE

$A$  : vehicle's cross-sectional area, m<sup>2</sup>  
BET : battery-electric truck  
 $C_d$  : aerodynamic drag coefficient  
 $C_{rr}$  : rolling resistance coefficient, kg/ton  
 $C_{rr\ avg}$  : average rolling resistance coefficient, kg/ton  
 $C_{rr\ drum}$  : rolling resistance coefficient on a drum, kg/ton  
 $C_{rr\ flatroad}$  : rolling resistance coefficient scaled to be equivalent to flatroad, kg/ton  
 $C_{tyre}$  : tyre heat capacity, J/kgK  
 $d_{SoC}$  : dynamic state of charge, %  
 $F_p$  : parasitic loss force, N  
 $F_r$  : propulsion force, N  
 $F_{res}$  : resultant force, N  
 $F_x$  : rolling resistance force, N  
 $F_z$  : vertical force, N  
 $g$  : gravitational acceleration, m/s<sup>2</sup>  
 $L$  : normal force offset, m  
 $M$  : braking moment, Nm  
 $m_{truck}$  : mass of truck, kg  
 $m_{tyre}$  : mass of tyre, kg  
 $P_{int}$  : internal and accessory power losses of vehicle, W

$P_r$  : propulsion power, W  
RR : rolling resistance  
 $R_{drum}$  : drum radius, m  
 $R_{tyre}$  : tyre radius, m  
 $R_{specific}$  : gas constant, J/kgK  
 $S_{range}$  : driving range, m  
 $t_{drive\ time}$  : drive time, s  
 $T_{amb}$  : ambient temperature, °C  
 $T_{tyre}$  : tyre temperature, °C  
TRR : transient rolling resistance  
 $V$  : vehicle speed, m/s  
 $W_{bat}$  : battery capacity, W  
 $Q$  : amount of energy needed to heat rubber, J  
 $\alpha$  : road inclination, %  
 $\eta_{pt}$  : powertrain efficiency  
 $\Phi$  : relative humidity  
 $\rho_{air}$  : air density, kg/m<sup>3</sup>

## 1. INTRODUCTION

Global warming due to the increasing amount of greenhouse gases is a large problem for modern society. Vehicles produce carbon dioxide, which contributes to global warming and is directly coupled to the energy losses in a vehicle. One of the largest parts of the energy losses for trucks is caused by tyre rolling resistance (RR). It has been

\*Corresponding author. e-mail: jahyt@kth.se

shown with vehicle testing that low rolling resistance tyres correlate with fuel consumption (Surcel and Michaelsen, 2010). Furthermore, the understanding of rolling resistance at cold temperatures and the transient behaviour of the tyre is an increasingly interesting area of research because of the transition to a new generation of battery-electric trucks (BET). Vehicle manufacturers must be able to provide sufficient driving range in warm as well as cold environments, while expensive batteries dictate the price of BETs. In Europe, to obtain the UNECE R117 label (Amendment of Rolling Resistance in R117, 2009) the tyre manufacturers are mandated to test rolling resistance on a drum according to the ISO 28580 (2009) test standard. To homologate differences between different measurement rigs (Amendment of Rolling Resistance in R117, 2009) correction equations for room temperature and drum diameter are introduced in the standard. This test method takes a snapshot of the stabilised rolling resistance at +25 °C ambient temperature after stabilised rolling resistance has been established where the warm-up phase lasts 3 hours. This is a convenient method to compare RR but in real road applications, rolling resistance is much more complex. Difficulties arise when label values are used in energy consumption analyses. A large drawback of the ISO 28580 test standard is that it does not take into account variations of ambient temperature or transient rolling resistance (TRR). Other test standards exist such as SAE J1269 and SAE J2452, which of SAE J2452 considers also vehicle speed (stepwise coast-down method) (Wen *et al.*, 2014). However, also this test standard neglects the effects of transient rolling resistance and different ambient temperatures. Recently the European Commission has developed a CO<sub>2</sub> simulation tool (VECTO) for heavy-duty vehicles (EC, 2019). It also uses constant rolling resistance values as an input and disregards the effect of ambient temperature on RR and TRR. To improve the correlation between the energy consumption in real operational conditions and estimates using various simulation tools, there is a need for more data of rolling resistance at various ambient temperatures and different operating conditions.

Viscoelasticity in rubber accounts for the dominant part of rolling resistance (80 ~ 95 %) (Aldhufairi and Olatunbosun, 2018), while adhesion, sliding and aerodynamic losses account for the remaining part (Nakajima, 2019). It is a well-known fact that filler reinforced rubber has a considerable temperature dependency on stiffness and dissipation properties and therefore on rolling resistance (Greiner *et al.*, 2018). However, extensive experimental RR studies or finite element simulations at cold ambient temperatures are lacking for truck tyres. Making a universal simulation model for RR is challenging due to multiple different usage factors and parameters affecting RR such as inflation pressure (Aldhufairi and Olatunbosun, 2018), axle loads, road softness (Wong, 2001) and surface roughness (Yokota *et al.*, 2012), wheel alignment, tyre temperature

(Nielsen and Sandberg, 2002), driving torque, slip angle (Schuring, 1976) and many more.

A measurable reduction of the rolling resistance by reducing the airflow around the tyre was shown by Oswald and Browne (1981). They suggested that building an encapsulation for the tyre might reduce rolling resistance. Bode (2020) showed with experimental testing a noticeable reduction of RR with encapsulation around a truck tyre. This could prove to have an even higher effect at very low temperatures. He also noted a significant increase in rolling resistance with rain, as did Ejsmont *et al.* (2015) for a passenger car tyre. In another study, Ejsmont *et al.* (2018) studied the effect of ambient temperature on truck tyres between +4 °C and 38 °C. They noted that measurements performed in temperatures deviating from standard temperatures should be corrected using some kind of correction equation.

Even though rolling resistance is a widely researched area, there is a lack of knowledge in transient rolling resistance, especially at cold temperatures. Current regulations drive the tyre manufacturers to optimise tyre RR at +25 °C, which might not result in the best compromise between all the different parameters. Many countries have an average yearly temperature that is far from +25 °C. As an example, one of the warmest countries in Europe, Italy, has a yearly average temperature of 13.5 °C while one of the colder countries of Europe, Finland, has an average temperature of 1.7 °C (Average yearly temperature (1961-1990, Celsius) - by country).

The novelty of this research is quantifying rolling resistance changes of a regional 315/70 R22.5 heavy truck tyre at different ambient temperatures (-30 to +25 °C) using a state of the art climate wind tunnel. The change of the rolling resistance due to water cooling was measured at +25 °C. Furthermore, the study shows the effect of temperature on a hypothetical BET with varying rolling resistance and air density as a function of ambient temperature. The article provides a better understanding of the temperature dependency of rolling resistance, which helps to dimension batteries of electric trucks or to create transient rolling resistance models that take into account tyre or ambient temperature.

The outline is the following: firstly, the basics of the rolling resistance are covered. Secondly, the test setup is described. Thirdly, results and range calculations are shown with varying rolling resistance, air density and relative humidity. Finally, conclusions and future work are presented.

## 2. ROLLING RESISTANCE

Most of the rolling resistance is related to the viscoelastic behaviour of filled rubber when strain is imposed while rolling. Viscoelasticity can be explained as different loading and unloading curves as illustrated in Figure 1. In a rolling

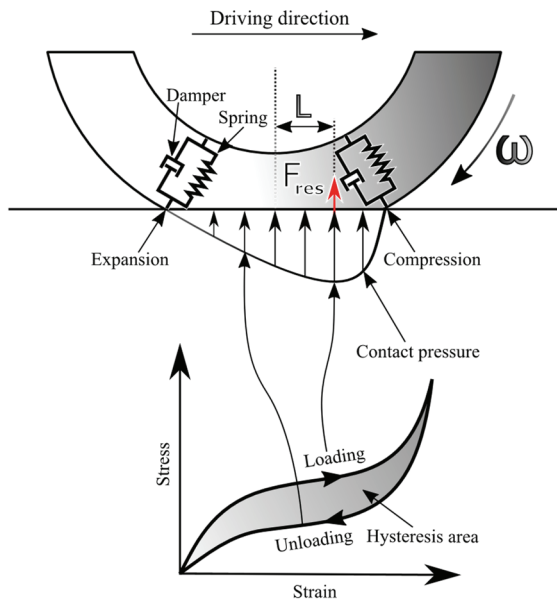


Figure 1. Asymmetric contact pressure is caused by the viscoelasticity in filler reinforced rubber when a tyre is rolling.

motion, the rubber compresses at the leading edge of the tyre contact patch and expands at the trailing edge of the contact patch. These subsequent loading and unloading events form an asymmetric contact pressure that shifts the resultant force ( $F_{res}$ ) in front of the tyre rotation axis with an offset  $L$ . This shifted resultant force creates a braking moment ( $M = F_{res}L$ ), which is the largest part of the rolling resistance.

Viscoelasticity dissipates energy into heat warming up the tyre. This strain-induced heat affects rolling resistance in two ways: (I) with increasing temperature the molecular mobility of rubber increases causing a decrease in hysteresis area and (II) tyre pressure rises and decreases tyre deformation i.e. reduced strain-induced hysteresis. The tyre warms up until the strain-induced heating effect and cooling effects from the surrounding airflow and road reach a thermal balance. During this warm-up period rolling resistance is decreased considerably and is called transient rolling resistance. This article aims to quantify the effects of different ambient and tyre temperatures on transient and stabilised rolling resistance.

The widely acknowledged definition of rolling resistance is energy loss over unit distance,  $J/m$ , which also corresponds to the definition of force. Schuring (1980) proposed a rolling resistance definition where the rolling resistance force is fully converted into heat. Li and West (2019) demonstrated with continuum mechanics and finite element calculations that part of the energy goes to balance the mechanical work and the energy is not fully converted to heat. Although, they noted that this additional part cannot

be separated with experimental methods and thereby can only be differentiated from each other using simulation methods. The definition is backwards compatible with Schuring's definition. Here, the rolling resistance force is defined according to Schuring, energy consumed by unit distance.

There are multiple rolling resistance test methods: force, torque, power and coast-down (deceleration). In all of the previously mentioned methods, the measured quantity is converted to a force at the tyre/drum or tyre/road interface. The time-dependent unitless rolling resistance coefficient  $C_{rr}(t)$  is usually related to the axle load and can be calculated with the force method followingly:

$$C_{rr}(t) = 1000 \frac{F_x(t) - F_p}{F_z}, \quad (1)$$

where  $F_x$  is the longitudinal force at the drum/tyre interface,  $F_z$  is the vertical force,  $F_p$  is the parasitic loss force.  $C_{rr}$  is scaled by a thousand so that units become  $kg/ton$ . This is usually done for easier readability of the  $C_{rr}$  values. In the present study, the parasitic losses are defined as losses coming from the drum bearings and the measurement device itself. Alternative definitions for parasitic losses do exist (ISO 28580, 2009).

Multiple experimentally defined empirical regression models exist for the rolling resistance that is a function of vehicle speed or tyre pressure. An example of a least-square regression model for light-truck tyres is used in SAE J2452 (Nakajima, 2019). It has three empirical coefficients and is a function of vehicle speed, axle load and tyre pressure. The drawback of these models is that they have applicability only in stationary conditions. Some models such as Greiner *et al.* (2018), have taken into account transient rolling resistance. The Greiner model takes tyre inner-liner temperature and vehicle speed as input. This model has yet to be proven to be extended to work with truck tyres. Additionally, it should be extended to work at different ambient temperatures.

### 3. TEST SETUP

In this section, the test setup is introduced for dry and wet tests. The tests were conducted at Scania's climate wind tunnel where the ambient temperature can be altered. In common RR measurement methods, the cooling effect of wind is not included. More information on this wind tunnel can be found from Duell *et al.* (2016). The measurement drum has a diameter of 2.5 m, which is 0.5 m larger than the recommended diameter in the ISO 28580 standard (2009). This is beneficial for the measurements because a larger diameter warms up the tyres less and mimics a flat road better. If the drum diameter is too small, the tyre temperature becomes too high and the measurement results might become less relevant. There are multiple different

approximation equations to convert drum measurements ( $C_{rr\_drum}$ ) to flat road results ( $C_{rr\_flatroad}$ ) such as the widely known Clark’s formula (Clark and Dodge, 1979):

$$C_{rr\_flatroad} = \frac{C_{rr\_drum}}{\sqrt{1 + \frac{r_{tyre}}{r_{drum}}}} \quad (2)$$

where  $r_{tyre}$  and  $r_{drum}$  are the tyre and drum radius respectively. All the measurements shown in this article are direct drum tests and no conversion equations were used here so that readers can use the equation of their choice to scale results to a flat road. However, if Clark’s formula would be used in this case the results should be scaled with the factor of 0.84 ( $r_{tyre} = 0.504$  m,  $r_{drum} = 1.25$  m) to be equivalent to a flat road. The wind and drum speed were set to 80 km/h and the tests were conducted at different ambient temperatures (+25, +5, -15, -30 °C). To make it relevant to measure the tyre in such a large temperature range, the chosen tyre has a Mud + Snow (M+S) and Three Peak Mountain Snow Flake (3PMSF) marking for winter usage. Dual tyres were used on the measured axle. Figure 2 illustrates the measurement steps. The measured tyres have a 5.1 kg/ton labelled rolling resistance value (class C rolling resistance (European Union (EU), 2009)).

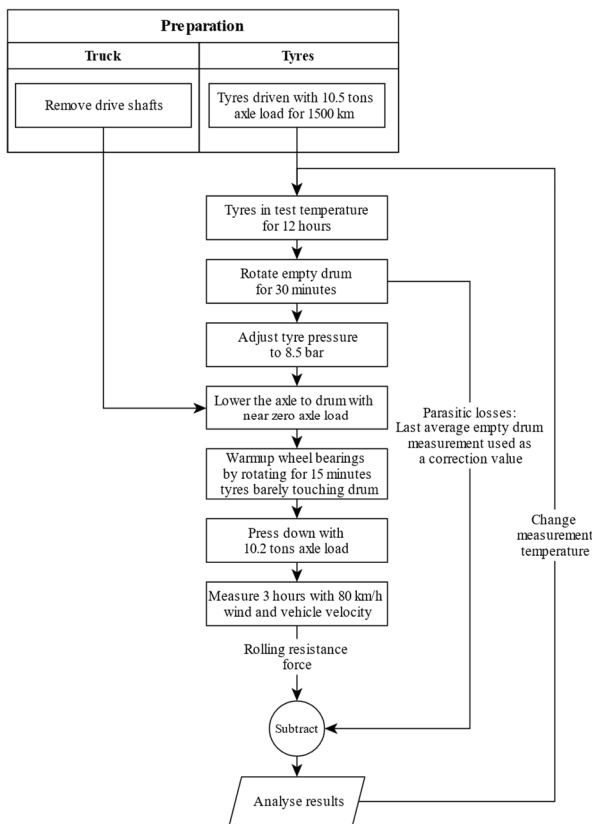


Figure 2. Measurement flow chart.

Before the tests, the tyres were preconditioned by driving them 1500 km using 10,500 kg axle load and 8.5 bar inflation pressure. This was done so that the measurements would show the actual RR instead of evaluating the reduction of RR because of strain-softening (Mullins effect) (Diani *et al.*, 2009) in new tyres. To measure the tyre temperature the tyres were equipped with K-type thermocouples that were glued into drilled holes located at the tyre shoulder and near the apex, which are shown in Figure 3 (left). To achieve a homogeneous temperature distribution throughout the tyre, the tyres were kept in the measurement temperature for at least 12 hours before starting the tests.

The drive shafts were removed during the tests to separate tyre RR from the gearbox and differential losses. Before the start of every test, the truck was lifted with an overhead crane and the drum was driven for 30 minutes (80 km/h) to warm up the drum bearings and stabilise the force measurement. The last averaged value of the drum rolling loss was subtracted afterwards from the rolling resistance measurements to remove most of the parasitic losses from the drum bearings. After this, the drive axle was lowered on the drum so that the tyres were barely touching the drum and driven for 15 minutes. This step was done to warm up the wheel bearings. Finally, the tyre pressure was adjusted to 8.5 bar, the axle was lowered on the drums and 10.2 tons axle load was applied on the drive axle. These steps were repeated in all of the measurement temperatures. This means that the measured rolling resistance includes the losses from the wheel bearings and the aerodynamic resistance of the tyre. The effects of these are however estimated to be considerably lower than the rolling resistance caused by the viscoelastic effects (Nakajima, 2019). More work could be done to understand the amount of truck wheel bearing losses at different temperatures. The measurements here are by no means attempted to be equivalent to ISO 28580 RR tests, because of the larger cooling effect of the wind and measurement from the truck axle. Slight misalignment of the axle might affect results by some amount. Additionally, parasitic losses are defined



Figure 3. Truck measurement setup with thermocouple temperature sensors drilled into a tyre (left) and water spraying nozzle in front of the tyre (right).

slightly differently than in ISO 28580 (2009). Nevertheless, the results at +25 °C do not differ significantly from the ISO results.

The change of rolling resistance in wet driving conditions was measured by spraying water on the tyres. During the rain/wet tests, 0.2 l/s water was sprayed to the left tyres at 80 km/h vehicle speed (Figure 3 right). Ejsmont *et al.* (2015) have conducted flat road measurements for a passenger car tyre in rainy weather and concluded that a large part of the increase in rolling resistance in their tests was due to hydrodynamic effects i.e. pumping a water layer away from the contact patch. They used infrared measurements from the sidewall. However, as later on shown in this article, the positioning of the temperature sensors have a large effect on the conclusions drawn from the measurements. Rubber has the highest temperatures at the inside of the volume which is why it is possible that the measurements inside of the tyre are a better indicator for tyre RR. In the present work, the hydrodynamic effects are considered to be close to zero because of the relatively low amount of water spraying and the usage of the outer drum measurements where the water layer build-up is less likely than using flat surface measurements.

Figure 4 shows a truck in the test cell at -30 °C ambient temperature where the tyre is considerably warmer than the surroundings. It is noteworthy to remark that the drum surface does not cool down to the test cell ambient temperature, as can be seen from Figure 5. This is because a large part of the measurement drum is in the basement and the basement has approximately +15 to +25 °C temperature. Especially in cold weather, the difference between the cell temperature and drum temperature is close to 20 °C. Yokota *et al.* (2012) made quasi-static finite element simulations for a passenger car tyre and attempted to quantify the effect of road surface and ambient temperature on the tyre temperature. Radiation was not taken into account in their study. They concluded that both road and ambient temperature have an impact on the tyre's internal temperature. However, they found that road temperature has a larger sensitivity on the tyre temperature than the

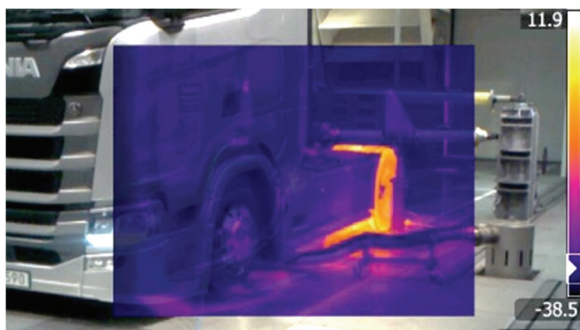


Figure 4. Tyre temperature after testing at -30 °C measurement temperature.

surrounding temperature. Thereby, the difference in ambient/drum temperature might have a reducing effect on the measured rolling resistance values at cold temperatures in this article.

4. TEST RESULTS

The results from the tests are discussed in this section. The transient rolling resistance starts with a higher value and reaches a lower stabilized  $C_{rr}$  roughly after 45 ~ 80 minutes as shown in Figure 6 (upper). With decreasing temperature, the rolling resistance increases. It should be noted that in Figure 6 (upper) and Figure 15 (lower) at the coldest temperature the rolling resistance increases slightly from 90 ~ 155 minutes which can be explained with the drop of measurement cell temperature at the same time from -27 to -31 °C (Figure 6 lower).

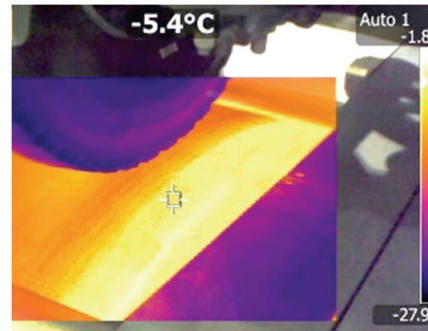


Figure 5. Measurement drum at -30 °C before the start of measurement. The drum is warmer than the surrounding temperature.

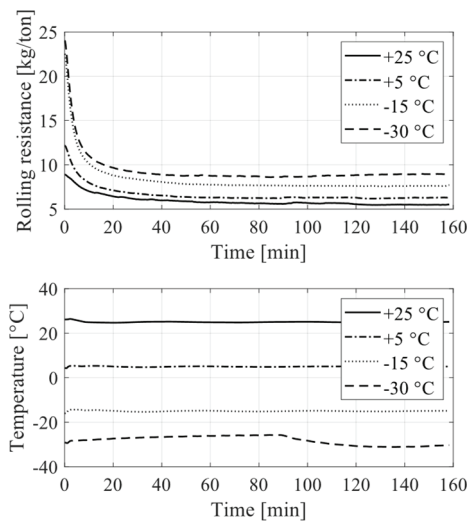


Figure 6. Rolling resistance plotted over time at different ambient temperatures (upper); Test cell temperature during the tests (lower).

Figure 7 shows the rolling resistance measurements normalised with the measured stabilised  $C_{rr}$  value at +25 °C. At -15 °C and -30 °C the initial rolling resistance is over four times the stabilised RR at +25 °C. At -30 °C, the stabilised RR is approximately 1.65 larger compared to the values at +25 °C.

The stabilised temperature difference between the tyre shoulder and ambient temperature has a nearly linear relationship with ambient temperature (Figure 8), while the stabilised rolling resistance as a function of ambient temperature has a nonlinear relationship (Figure 9). An increase in tyre temperature during driving directly indicates that the tyres dissipate a larger amount of energy.

Rolling resistance seems to have a strong correlation with the tyre shoulder temperature as found in Figure 10. In all the temperatures the shoulder temperature/RR plots create graphs with a form similar to  $\tan \delta$  (loss angle) plots in dynamic mechanical analysis plotted as a function of

temperature (Rodgers, 2020). A tyre is made of many different rubber compounds so the plot is similar but in some meaning describes the dissipation of weighted average response from all rubber compounds combined with the increase of the tyre pressure at the same time. However, temperature measurements near the apex seem to be an insufficient indicator for the rolling resistance (Figure 11). Nevertheless, both of the measurements show that by having a higher tyre temperature the rolling resistance is reduced significantly, affecting the energy consumption of the vehicle.

Figure 12 shows the temperature warm up inside the tyre shoulder and near the apex. What can be seen is that the shoulder measurements reach higher temperatures than the apex measurements. The warmup trend can be further on highlighted with a logarithmic plot in Figure 13. What stands out is that the apex temperatures have a delayed response and reach steady temperature slower compared to

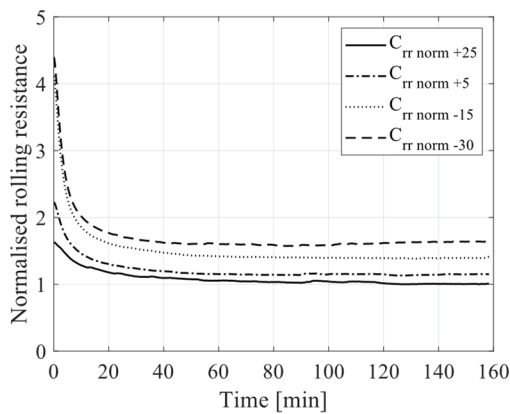


Figure 7. Rolling resistance normalised with stabilised RR value at +25 °C.

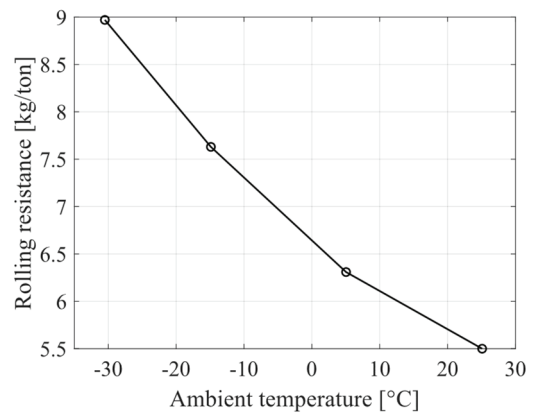


Figure 9. Stabilised rolling resistance plotted over different ambient temperatures.

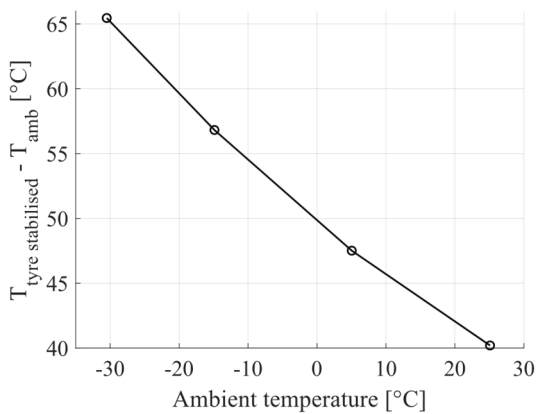


Figure 8. Stabilised difference between ambient and tyre temperature.

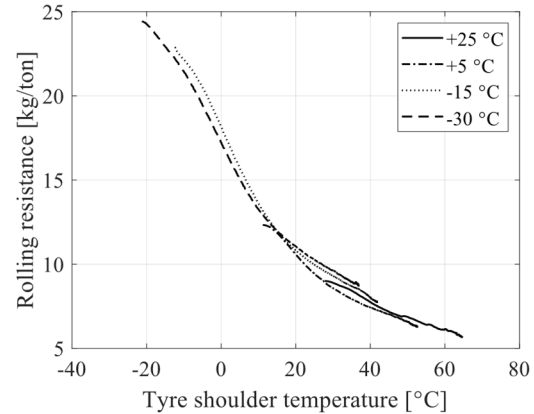


Figure 10. Rolling resistance is plotted over tyre temperature at the tyre shoulder.

the tyre shoulder temperature. There are three likely explanations for this: Firstly, the sensor is located closer to the rim, which could act as a heat sink. Secondly, it is not possible to drill as deep holes near the apex as in the tyre shoulder without puncturing the tyre. Thirdly, there simply might be less energy dissipation near the apex than at the tyre shoulder.

Not only does the tyre temperature converge to a lower temperature when the ambient temperature decreases (Figures 12 and 13) but also the differences between the tyre ( $T_{tyre}$ ) and ambient temperature ( $T_{amb}$ ) increase with decreasing ambient temperatures as highlighted in Figure 14. This is another indicator that more energy ( $Q$ ) must be put into the tyre to heat a large mass of rubber ( $m_{tyre}$ ) with a certain heat capacity ( $C_{tyre}$ ) up to a higher temperature difference ( $Q(T) = C_{tyre} m_{tyre} (T_{tyre} - T_{amb})$ ).

The transient part of the rolling resistance could be presented as an average rolling resistance over a certain drive time at different temperatures, which would be a more

meaningful value to compare in range calculations without actually modelling the transient rolling resistance. To get a more representative value of the rolling resistance for a given long haulage drive cycle, an averaged rolling resistance over a certain drive time,  $C_{rr\_AVG}(t)$ , is proposed according to Equation (3).

$$C_{rr\_AVG}(t) = \frac{1}{t_{drive\_time}} \int_{t=0}^{t_{drive\_time}} C_{rr}(t) dt \quad (3)$$

where  $t_{drive\_time}$  is the length of the driving time. Due to the long duration of the TRR, it becomes significant for vehicle energy consumption. An averaged rolling resistance plot gives an insight into the real-life rolling resistance at different drive times. Figure 15 shows both the actual and averaged rolling resistance for a given drive time at different temperatures. As an example, driving 50 minutes

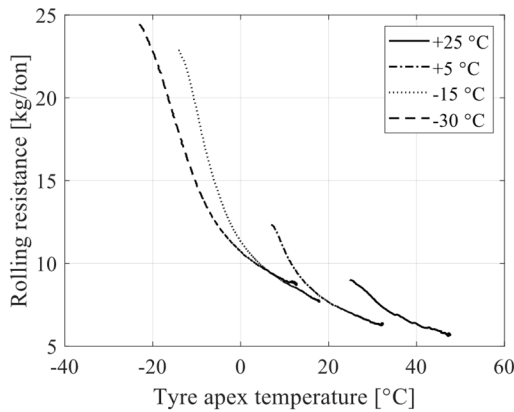


Figure 11. Rolling resistance is plotted over tyre temperature at the apex.

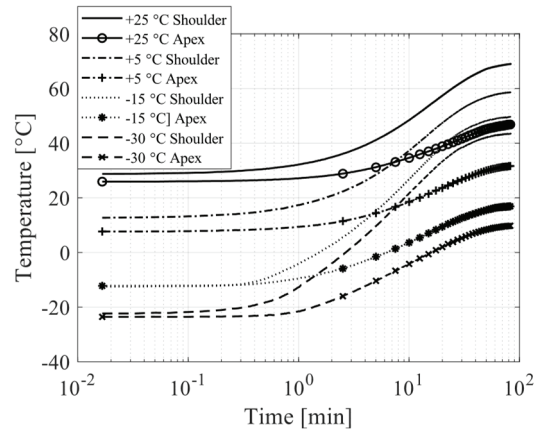


Figure 13. Tyre shoulder and apex temperatures plotted over a logarithmic time scale. The apex temperature has a delayed response and warms up at a slower pace than shoulder temperature.

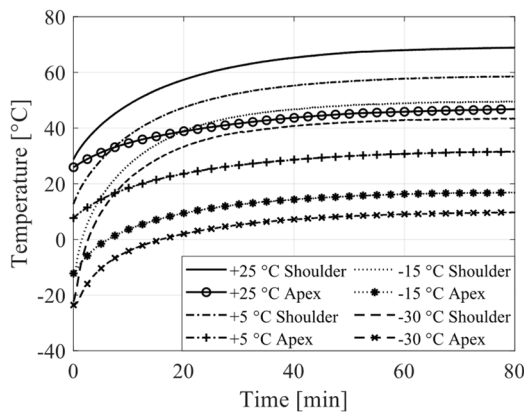


Figure 12. Tyre shoulder and apex temperatures plotted.

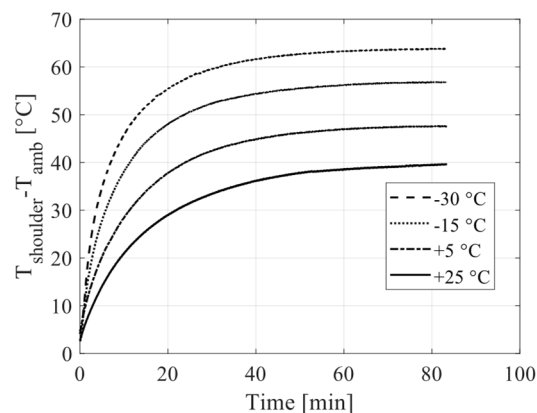


Figure 14. Difference between tyre shoulder temperature and ambient temperature.

at  $-30\text{ }^{\circ}\text{C}$  the average rolling resistance would be  $\sim 1.7\text{ kg/ton}$  higher than the current  $C_{rr}(t)$  value. The proposed average rolling resistance plots can be extracted with commonly used testing methods used according to the ISO 28580 (2009) EU labelling except for the coast-down method. It is noteworthy to mention that at the end of the measurement, the difference between  $C_{rr\_AVG}$  and  $C_{rr}$  at  $-30\text{ }^{\circ}\text{C}$  is lower than at  $-15\text{ }^{\circ}\text{C}$ . This is because of the slight decrease in ambient temperature at the end of  $-30\text{ }^{\circ}\text{C}$  measurements (Figure 5) resulting in an increase of  $C_{rr}$  values, which can be seen from Figure 15.

The comparison between wet and dry tests are shown in Figure 16. The tests start from a similar rolling resistance but the dry measurements converge into approximately

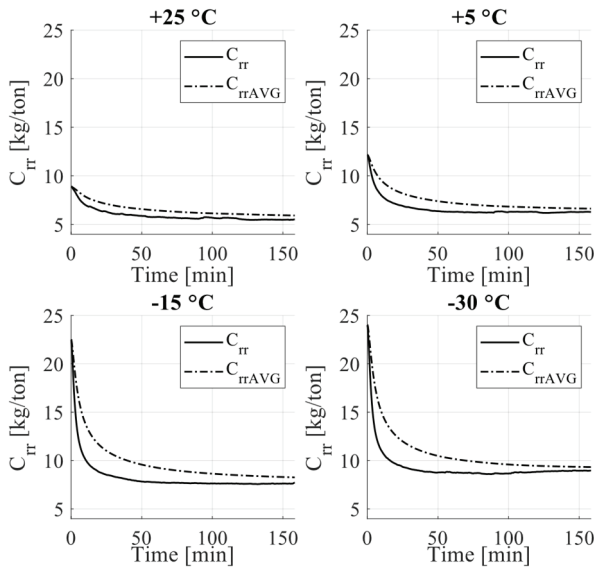


Figure 15. Current rolling resistance ( $C_{rr}$ ) and averaged rolling resistance ( $C_{rr\_AVG}$ ) over different drive times at different ambient temperatures.

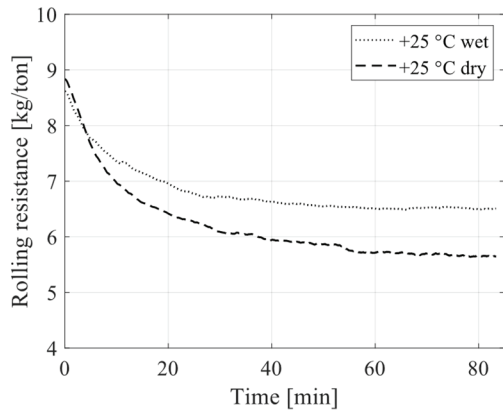


Figure 16. Rolling resistance with dry and wet driving conditions plotted over time.

15 % lower rolling resistance. The fact that both rolling resistance measurements start from similar values signals that there is not enough water spraying to generate a water layer that the tyre has to pump away from the tread. Therefore, it can be concluded that most of the increase in rolling resistance in this test is due to lower tyre temperature.

## 5. EFFECT OF RR ON BET DRIVING RANGE

To highlight the influence of ambient temperature on rolling resistance, simulations were conducted comparing the range of a hypothetical long haulage BET driving at a constant velocity of 80 km/h at different ambient temperatures. Following values are chosen for the range calculation: the battery size ( $W_{bat}$ ) is 600 kWh, the state of charge window ( $d_{soc}$ ) is 80 % (useable battery capacity), battery and the total powertrain efficiency ( $\eta_{pt}$ ) is 0.94, the aerodynamic drag coefficient ( $C_d$ ) is 0.5 and the cross-sectional area ( $A$ ) is  $10\text{ m}^2$ . For simplification, it is assumed that the vehicle has the same tyres at every axle with the same rolling resistance coefficient and the vehicle weight ( $m_{truck}$ ) is 40 tons. The average rolling resistance after driving 155 min ( $C_{rr\_avg}$ ) varies from 5.9 to 9.3 kg/ton depending on the ambient temperature. The force opposing the vehicle motion is calculated in the following way:

$$F_r = C_{rr\_avg}(T_{amb})m_{truck}g + \frac{1}{2}\rho_{air}(T_{amb}, \Phi)C_dAV^2 + m_{truck}\frac{dv}{dt} + m_{truck}g\sin\alpha + \frac{P_{int}}{V}, \quad (4)$$

where  $C_{rr\_avg}$  is a function of ambient temperature ( $T_{amb}$ ), the density of air ( $\rho_{air}$ ) is a function of both ambient temperature and relative air humidity ( $\Phi$ ),  $g$  is the gravitational acceleration and  $V$  is the vehicle velocity. For simplicity, it is assumed that the inclination of the road ( $\alpha$ ) and internal and accessory losses ( $P_{int}$ ) are zero. The vehicle is driving in a long haulage application, which is why the acceleration losses can be assumed to be near zero also. Both air density and rolling resistance are varied with respective temperatures. Dry air density is calculated as  $\rho(T_{amb}) = p / R_{specific}T_{amb}$ , ( $R_{specific} = 287.058\text{ J/kgK}$ ). Calculation and coefficients for the humid air are done using the method shown in Davis (1992). The needed propulsion power ( $P_r$ ) for the vehicle is calculated with:

$$P_r = \frac{F_r V}{\eta_{pt}} \quad (5)$$

The resulting range ( $S_{range}$ ) is calculated from:

$$S_{range} = \frac{d_{soc}W_{bat}V}{P_r} \quad (6)$$

Figure 17 shows the change of air density with 0 % and 100 % air humidity. Colder temperature causes considerably higher air density, which results in an increase of aerodynamic resistance. Above +15 °C the density with 100 % air humidity starts to diverge from the dry air density.

Figure 18 illustrates the effect of different ambient temperatures on the simulated BET range because of the change in rolling resistance according to the earlier shown average rolling resistance values (Figure 15 at  $t = 155$  min). The largest change is because of the change in rolling resistance (solid line). The change of air density plays also some role for the range (dashed-line), but there seems to be only a marginal difference between zero relative humidity and 100 % relative humidity (dashed-line with circles).

As can be seen, the range drops significantly with decreasing temperature. At a very cold temperature, -30 °C,

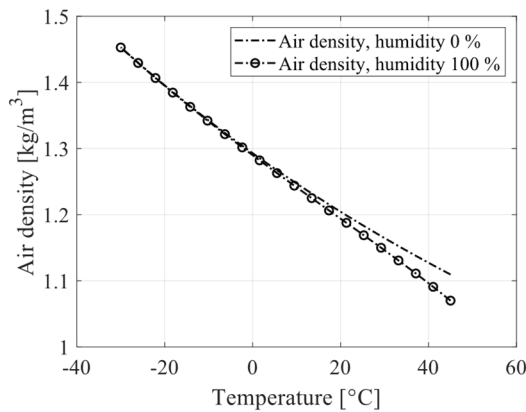


Figure 17. Change of air density when air humidity and temperature are varied.

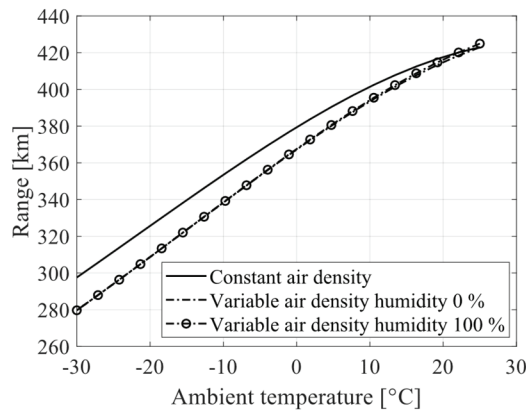


Figure 18. BET driving range when rolling resistance and air density is varied with 0 % and 100 % relative air humidity.

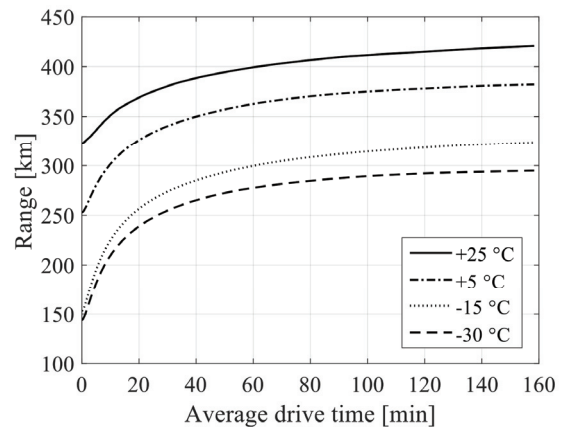


Figure 19. Range calculations with varying drive time at different ambient temperatures.

the range has dropped approximately 29 % from the range at +25 °C ambient temperature only because of the rolling resistance. When both rolling resistance and aerodynamic resistance is varied, the decrease in range is 34 %. Therefore, it is essential to take into account both the change of rolling resistance and the change of air density in range calculations, whereas the effect of air humidity on air density can be neglected. Additionally, the real range is decreased because of other aspects which are not taken into account here e.g. heating or cooling of the cabin and thermal management of batteries. The influence of an increase in air density at cold temperatures can be expected to be lower for vehicles equipped with internal combustion engines because of the increase in volumetric efficiency with higher air density (Di Battista *et al.*, 2018).

Figure 19 depicts the range that the vehicle can cover with different lengths of driving trips, where the averaged rolling resistance is varied depending on the drive time. As an example, if all the trips are only 20 minutes long and the tyres always have time to cool down fully between the stops, the vehicle could cover approximately 325 km distance at +5 °C. If the trips would be 160 minutes long at the same temperature the vehicle would have a 380 km range.

## 6. CONCLUSION

This article studied the temperature dependency of rolling resistance using a climate wind tunnel. To show the importance of the temperature dependency of rolling resistance, BET driving range calculations were provided. The insights gained from this study may be of assistance for truck and tyre manufacturers as well as when designing new standards and regulations. The findings can be summarised with the following remarks:

- (1) The results show a considerable increase of rolling

resistance at decreasing ambient temperatures.

- (2) Stabilised rolling resistance is dependent on the tyre temperature, which on the other hand is defined by the cooling effect of the ambient temperature.
- (3) The positioning of the temperature measurement is an important aspect for indicating rolling resistance. The tyre shoulder is a better indicator for rolling resistance than near the apex where the tyre warms up slower. Also cooling from the rim might play a role in this.
- (4) Even a relatively light water spraying increases rolling resistance by 15 % compared to the dry conditions at +25 °C due to lower operating temperature.
- (5) The results of this study indicate that the transient effect of rolling resistance should be taken into account in range calculations.
- (6) As a first step to getting more realistic values from the labelling tests, RR tests could be conducted at the average temperature of the continent where the tyres are used instead of at +25 °C.
- (7) For some applications, the transient part of the rolling resistance could be presented as an average rolling resistance over a certain drive time. This could be a more meaningful value to compare in range calculations without actually modelling the transient rolling resistance.
- (8) The effect of ambient temperature on rolling resistance is far too large to be ignored in energy consumption analyses of vehicles and especially for battery-electric trucks. Also, the change of air density affects the energy consumption of a BET.

This study has not taken into account different driving cycles, which are particularly important for urban and regional driving and should be studied more in the future. Transient rolling resistance models should be incorporated especially in distribution BET range and electric city bus battery size simulations. In the future, vehicles could be equipped with tyre temperature sensors that would indicate the current rolling resistance to estimate the remaining driving range more accurately. More work should be done to understand wheel-hub bearing losses at different temperatures and the warm-up behaviour of the tyre when driving torque is applied. Optimising airflow away from the tyre could prove to have a decreasing effect on rolling resistance, especially at low temperatures due to the lower cooling effect. It would be beneficial to design a rolling resistance measurement device that could decouple brakes and bearing losses from the measurements to gather real road data. Further studies regarding rolling resistance at various operating conditions should be conducted in the future.

**ACKNOWLEDGEMENT**—The authors would like to thank the Centre for ECO<sup>2</sup> Vehicle Design funded by the Swedish Innovation Agency Vinnova (Grant Number 2016-05195), the strategic research area TRENOP and Scania for financial support.

## REFERENCES

- Aldhufairi, H. S. and Olatunbosun, O. A. (2018). Developments in tyre design for lower rolling resistance: a state of the art review. *Proc. Institution of Mechanical Engineers, Part D: J. Automobile Engineering* **232**, **14**, 1865–1882.
- Amendment of Rolling Resistance in R117 (2009). Rolling Resistance Implementation in R117. Informal Document No. GRRF-66-28.
- Average yearly temperature (1961-1990, Celsius) - by country. Lebanese Economy Forum. Available at: <https://web.archive.org/web/20150905135247/http://lebanese-economy-forum.com/wdi-gdf-advanced-data-display/show/EN-CLC-AVRT-C/>
- Bode, O. (2020). Der Einfluss von Wärmeverlusten auf den Rollwiderstand von Reifen. FAT-Schriftenreihe 325.
- Clark, S. K. and Dodge, R. N. (1979). A Handbook for the Rolling Resistance of Pneumatic Tires. Technical Report UMR1216.
- Davis, R. S. (1992). Equation for the determination of the density of moist air (1981/91). *Metrologia* **29**, **1**, 67–70.
- Di Battista, D., Di Bartolomeo, M. and Cipollone, R. (2018). Flow and thermal management of engine intake air for fuel and emissions saving. *Energy Conversion and Management*, **173**, 46–55.
- Diani, J., Fayolle, B. and Gilormini, P. (2009). A review on the Mullins effect. *European Polymer J.* **45**, **3**, 601–612.
- Duell, E., Kharazi, A., Nagle, P., Elofsson, P., Soderblom, D. and Ramden, C. M. (2016). Scania's new CD7 climatic wind tunnel facility for heavy trucks and buses. *SAE Int. J. Passenger Cars-Mechanical Systems* **9**, **2**, 785–800.
- Ejsmont, J., Sjögren, L., Świczko-Żurek, B. and Ronowski, G. (2015). Influence of road wetness on tire-pavement rolling resistance. *J. Civil Engineering and Architecture* **9**, **11**, 1302–1310.
- Ejsmont, J., Taryma, S., Ronowski, G. and Swieczko-Żurek, B. (2018). Influence of temperature on the tyre rolling resistance. *Int. J. Automotive Technology* **19**, **1**, 45–54.
- European Commission (EC) (2019). Vehicle Energy Consumption calculation TOoL - VECTO. [https://ec.europa.eu/clima/policies/transport/vehicles/vecto\\_en](https://ec.europa.eu/clima/policies/transport/vehicles/vecto_en)
- European Union (EU) (2009). Regulation (EC) No 1222/2009 of the European Parliament and of the Council of 25 November 2009 on the labelling of tyres with respect to fuel efficiency and other essential parameters (Text with EEA relevance). Document 32009R1222.
- Greiner, M., Unrau, H. J. and Gauterin, F. (2018). A model for prediction of the transient rolling resistance of tyres based on inner-liner temperatures. *Vehicle System Dynamics* **56**, **1**, 78–94.
- ISO 28580 (2009). Passenger car, truck and bus tyres — Methods of measuring rolling resistance — Single point test and correlation of measurement results.
- Li, Y. and West, R. L. (2019). Rolling resistance revisited.

- Tire Science and Technology* **47**, **1**, 77–100.
- Nakajima, Y. (2019). *Advanced Tire Mechanics*. Springer Nature Singapore Pte Ltd., Singapore.
- Nielsen, L. and Sandberg, T. (2002). A new model for rolling resistance of pneumatic tires. *SAE Trans.*, 1572–1579.
- Oswald, L. J. and Browne, A. L. (1981). Airflow field around an operating tire and its effect on tire power loss. Report No. CONF-810206-35.
- Rodgers, B. (2020). *Tire Engineering: An Introduction*. 1st edn. CRC Press. Boca Raton, Florida, USA.
- Schuring, D. J. (1976). Energy loss of pneumatic tires under freely rolling, braking, and driving conditions. *Tire Science and Technology* **4**, **1**, 3–15.
- Schuring, D. J. (1980). The rolling loss of pneumatic tires. *Rubber Chemistry and Technology* **53**, **3**, 600–727.
- Surcel, M. D. and Michaelsen, J. (2010). Evaluation of tractor-trailer rolling resistance reducing measures. *SAE Paper No.* 2010-01-1917.
- Wen, B., Rogerson, G. and Hartke, A. (2014). Correlation analysis of rolling resistance test results from SAE J1269 and J2452. *SAE Paper No.* 2014-01-0066.
- Wong, J. Y. (2001). *Theory of Ground Vehicles*. 3rd edn. John Wiley & Sons, Inc., New York, NY, USA.
- Yokota, K., Higuchi, E. and Kitagawa, M. (2012). Estimation of tire temperature distribution and rolling resistance under running conditions including environmental factors. *SAE Paper No.* 2012-01-0796.

**Publisher's Note** Springer Nature remains neutral with regard to jurisdictional claims in published maps and institutional affiliations.